

Immobilizing affinity proteins to nitrocellulose: a toolbox for paper-based assay developers

Carly A. Holstein¹ · Aaron Chevalier^{1,2} · Steven Bennett¹ · Caitlin E. Anderson¹ · Karen Keniston¹ · Cathryn Olsen³ · Bing Li³ · Brian Bales³ · David R. Moore³ · Elaine Fu⁴ · David Baker² · Paul Yager¹

Received: 29 June 2015 / Revised: 6 September 2015 / Accepted: 15 September 2015 / Published online: 1 October 2015
© Springer-Verlag Berlin Heidelberg 2015

Abstract To enable enhanced paper-based diagnostics with improved detection capabilities, new methods are needed to immobilize affinity reagents to porous substrates, especially for capture molecules other than IgG. To this end, we have developed and characterized three novel methods for immobilizing protein-based affinity reagents to nitrocellulose membranes. We have demonstrated these methods using recombinant affinity proteins for the influenza surface protein hemagglutinin, leveraging the customizability of these recombinant “flu binders” for the design of features for immobilization. The three approaches shown are: (1) covalent attachment of thiolated affinity protein to an epoxide-functionalized nitrocellulose membrane, (2) attachment of biotinylated affinity protein through a nitrocellulose-binding streptavidin anchor protein, and (3) fusion of affinity protein to a novel nitrocellulose-binding anchor protein for direct coupling and

immobilization. We also characterized the use of direct adsorption for the flu binders, as a point of comparison and motivation for these novel methods. Finally, we demonstrated that these novel methods can provide improved performance to an influenza hemagglutinin assay, compared to a traditional antibody-based capture system. Taken together, this work advances the toolkit available for the development of next-generation paper-based diagnostics.

Keywords Paper-based assays · Protein immobilization · Protein engineering · Nitrocellulose

Introduction

The success of bioassays depends critically on the immobilization of affinity reagents to the assay substrate. For paper-based assays, the most common immobilization method has been direct, physical adsorption of the affinity reagent to the assay membrane. This approach has worked well for a decade-long history of lateral flow tests, dot blots, and even more recent paper-based diagnostic technologies [1–3]. The success of direct adsorption in these assays has largely been due to the suitability of immunoglobulin G (IgG) antibodies to this process, which have been the mainstay of capture agents for lateral flow immunoassays [3–5]. However, as new paper-based assays are designed with non-antibody affinity reagents, the tried-and-true method of direct adsorption may no longer serve as the most effective method for immobilization.

Recombinant affinity proteins represent a useful class of affinity reagents that have thus far been under-utilized in paper-based diagnostics. Not only can these affinity proteins be designed to recognize a specific epitope of interest, but they can also be expressed recombinantly in bacterial cells, making them a simpler, lower-cost alternative to the monoclonal IgG

Published in the topical collection *Fiber-based Platforms for Bioanalytics* with guest editors Antje J. Baeumner and R. Kenneth Marcus.

Electronic supplementary material The online version of this article (doi:10.1007/s00216-015-9052-0) contains supplementary material, which is available to authorized users.

✉ Carly A. Holstein
cholst@uw.edu

¹ Department of Bioengineering, University of Washington, 3720 15th Ave NE, Seattle, WA 98105, USA

² Department of Biochemistry, University of Washington, 1705 NE Pacific St., Seattle, WA 98195-7350, USA

³ General Electric Global Research Center, 1 Research Cir, Niskayuna, NY 12309, USA

⁴ School of Chemical, Biological, and Environmental Engineering, Oregon State University, 103 Gleeson Hall, Corvallis, OR 97331, USA

antibodies customarily used in lateral flow-based diagnostics [6]. Additionally, recombinant affinity proteins can be fully customized from their genetic sequences, allowing the proteins to be optimized for many properties, including attachment to the assay substrate.

Here, we have leveraged the customizability of recombinant affinity proteins to develop novel strategies for the immobilization of these proteins to nitrocellulose for use as capture agents in lateral flow-based assays. As part of a project aimed at improving today's rapid influenza lateral flow tests, we used recombinant affinity proteins that have been computationally designed to bind sensitively and specifically to the stem region of the influenza surface protein hemagglutinin (HA) [7, 8]. We first characterized the use of direct adsorption for these "flu binders," which has proven not to be an effective method of immobilizing these small, recombinant affinity proteins. The lack of direct adsorption efficacy motivated the development of three novel methods for affinity protein immobilization: (1) covalent attachment through an epoxide-thiol linkage using a functionalized nitrocellulose membrane, (2) streptavidin-biotin linkage using a commercially available nitrocellulose-binding mutant streptavidin, and (3) coupling to a novel nitrocellulose-binding anchor protein through genetic fusion (see Fig. 1). All immobilization systems were evaluated on the basis of two metrics: immobilization efficiency and protein binding functionality as a capture agent for an influenza HA assay. We also compared these assay systems to a traditional antibody-based assay using direct adsorption of IgG to the nitrocellulose membrane using available off-the-shelf components.

Similar immobilization approaches have been demonstrated for countless other assay types, including protein microarrays and biochips [9–11], cellulose-based assays [12–15], and

microfluidic devices [3]. To our knowledge, these approaches have not been developed and demonstrated for nitrocellulose-based lateral flow assays, particularly for the immobilization of recombinant affinity proteins. The novel methods described herein are therefore expected to expand the toolkit for developers of nitrocellulose-based lateral flow tests and paper-based diagnostics.

Materials and methods

Recombinant flu binder preparation

In this work, three different versions of the previously developed [7, 8] flu HA binder (*Hemagglutinin Binder*) were used as base proteins: HB80.4 (8.7 kDa), HB36.5 (13.0 kDa), and HB36.6 (13.3 kDa). The HB80.x and HB36.x proteins are based on different scaffolds, but bind to the same stem region epitope of influenza HA [7, 8]. HB36.6 represents an iteration of HB36.5 that was further improved for stability and binding affinity [unpublished data under review for publication]. The amino acid sequences for HB80.4 and HB36.5, and the modifications developed herein, are provided in the [Electronic Supplementary Material \(ESM\)](#).

The recombinant influenza HA binders and nitrocellulose-binding anchor proteins were cloned, expressed in *Escherichia coli*, and purified via metal affinity chromatography using Ni-NTA resin to recognize C-terminal His tags, as described previously [7, 8]. All flu HA binders contained N-terminal FLAG tags to aid visualization of the proteins when needed. Biotinylated versions of the proteins were created by the addition of a C-terminal AVI tag at the genetic level, and enzymatic biotinylation of the AVI tag after protein expression and purification using the biotin protein ligase BirA, as described previously [7, 8]. This results in flu HA binders with a single biotin moiety per molecule to enable site-specific immobilization to a streptavidin-coated surface. Thiolated versions of the binders were created by mutating a select amino acid residue to cysteine, introducing a single thiol moiety for site-specific immobilization to a thiol-reactive surface. In both cases, the sites of the additions or mutations were analyzed and optimized using the Rosetta software suite (www.rosettacommons.org) to minimize impact on the binding functionality of the protein.

Membrane preparation

Nitrocellulose membranes were cut into test strips or multi-legged devices using a CO₂ laser cutter (Universal Laser Systems, Scottsdale, AZ). In most cases, each test strip was 3 mm wide by 24 mm tall. Generally, sets of 4 strips were cut together and connected by a 6-mm-tall section at the top of the device in order to promote batch processing. The distance

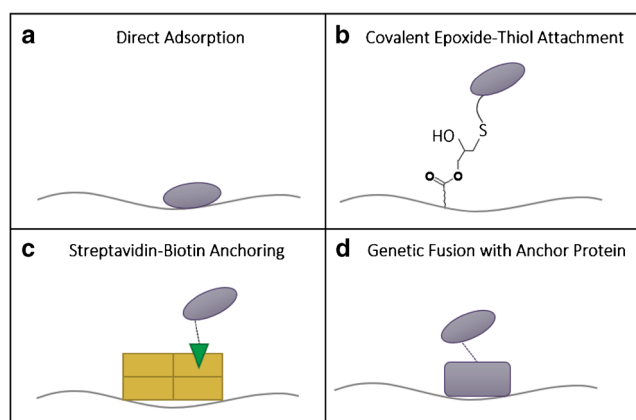


Fig. 1 Illustration of the four immobilization strategies developed and characterized in this work. **(A)** Direct adsorption of affinity protein to nitrocellulose. **(B)** Covalent attachment of thiolated affinity protein to GMA-modified nitrocellulose. **(C)** Anchoring of biotinylated affinity protein to streptavidin (regular and nitrocellulose-binding mutant version). **(D)** Genetic fusion of affinity protein to custom nitrocellulose-binding anchor protein

between strips was 6 mm designed to allow each set of strips to fit into the wells of a 96-well plate. In the case of the nitrocellulose-binding protein screening, 0.8 cm wide by 5 cm tall strips were used instead. Depending on the specific experiment, nitrocellulose membranes from either GE (FF60 or FF80HP, GE Healthcare, Amersham, UK) or Millipore (HFB135, Millipore, Billerica, MA) were used for testing. For the covalent attachment system, custom modified membranes were used, as described.

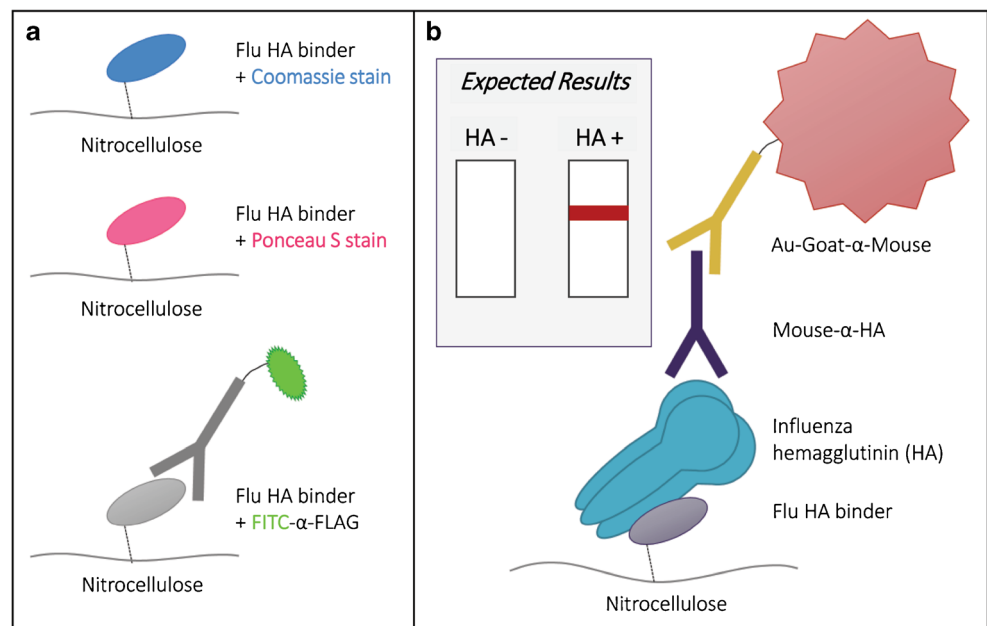
Commercially available proteins were purchased from the manufacturers as noted. Recombinant flu binder proteins were prepared as described above. Unless otherwise noted, all proteins were deposited onto the membrane strips using a piezoelectric printer (sciFLEXARRAYER S3, Scienion AG, Berlin, Germany). Proteins were prepared at 100 μ M in HBS (10 mM HEPES, 150 mM NaCl, pH 7.4) or PBS (10 mM sodium phosphate, 138 mM NaCl, 2.7 mM KCl, pH 7.4), unless otherwise noted. To avoid clogging the printer plumbing with particulate from the samples, all protein solutions were filtered through a centrifugal filter device with 0.2- μ m nylon membrane (VWR, Radnor, PA) at 6000g for 5 min prior to spotting. Test lines were created by 12 spots spaced 250 μ m apart, with 30 droplets per spot, and two passes were printed for each test line to saturate the membrane region. Each droplet was 450–500 pL, resulting in test lines comprising \sim 300 nL of protein solution in total. For the nitrocellulose-binding protein screening, circular spots were deposited using 1000 droplets at 450–500 pL per droplet for \sim 500 nL in total. After spotting, membranes were stored under desiccation at least overnight, and up to 1 week, before use.

Immobilization efficiency testing: lateral flow challenge

To screen the efficiency of each immobilization method, we used a lateral flow challenge system to evaluate how strongly a protein was immobilized to the membrane and to what extent it was subject to stripping by a challenge solution [16]. For the lateral flow challenge, strips were placed into a well (96-well plate for 3-mm-wide strips, multi-channel pipette reservoir for 0.8-cm-wide strips) filled with the given challenge solution (50 μ L and 5 mL, respectively). A cellulose absorbent pad (Millipore #CFSP223000) cut to the width of the device and 70 mm tall was secured to the top of the nitrocellulose device to aid wicking, either with tape or with a custom-made plastic housing. The challenge solution was allowed to wick through the strips for 15 min, at which point the strips were removed from the solution. In this work, challenge solutions included deionized H₂O, phosphate-buffered saline (PBS, pH 7.4, Sigma-Aldrich, St. Louis, MO) and PBS+0.1 % v/v Tween-20 (PBST).

The amount of protein remaining on the membrane was visualized in one of three ways, as illustrated in Fig. 2A: staining with a specific FITC-labeled anti-FLAG tag antibody, nonspecific protein staining with Coomassie Brilliant Blue (Thermo Scientific #20278, Life Technologies, Carlsbad, CA), or nonspecific protein staining with Ponceau S (Thermo Scientific #24580). For Coomassie staining, each membrane was incubated for 10 min with stain solution, followed by 10 min with destain solution, both with shaking. This protocol, adapted from Metkar et al. [17], uses a destain solution of 50 % H₂O, 40 % methanol, and 10 % glacial acetic acid, and a stain solution of 0.0025 % w/v Coomassie Brilliant Blue in destain solution. For Ponceau S staining, each membrane

Fig. 2 Illustrations of the methods used to assess each immobilization strategy. **(A)** Immobilization efficiency was tested via lateral flow challenge and protein staining with Coomassie Brilliant Blue, Ponceau S, or FITC-anti-FLAG tag. **(B)** Flu binder functionality was tested as a capture agent for a flu HA assay, using an antibody detection system with a monoclonal mouse-anti-HA primary antibody and a gold-conjugated goat-anti-mouse secondary antibody



was incubated with shaking for 5 min with stain solution (0.1 %w/v Ponceau S in 5 % acetic acid), followed by 2 min with H₂O for destaining, as based on the manufacturer's protocol and optimized in-house. In both cases, the stained devices were taped to a standard piece of printer paper and imaged at 48-bit HDR color, 600 dpi, $\gamma=1$ using a desktop scanner (Perfection V700 Photo Scanner, Epson, Long Beach, CA).

In the case of FITC-anti-FLAG tag staining, this fluorescently labeled antibody was used to specifically recognize the FLAG tag present in the recombinant HA binders. In these experiments, FITC-anti-FLAG (Sigma-Aldrich #F4049) was diluted to a working concentration of 100 $\mu\text{g}/\text{mL}$ in fetal bovine serum (FBS, Gibco #16000-077, Life Technologies), which prevents the antibody from adsorbing nonspecifically to the membrane. This FITC-anti-FLAG solution was then applied to the strips via lateral flow using 20 μL of solution per well of a 96-well plate, followed by a rinse with 40 μL buffer (PBS). The resulting fluorescently stained membranes were visualized by imaging under ultraviolet (UV) excitation using a commercial UV gel imager (Gel Doc EZ System, Bio-Rad, Hercules, CA). This imager utilizes a UV sample tray (Bio-Rad #170-8271) to achieve UV illumination of the membrane from broadband light, with the strength of fluorescence signal being controlled by the time of exposure. Membranes were imaged backing-side-up, as this orientation was determined to give the lowest background fluorescence.

Protein functionality testing: flu HA assay

Since protein immobilization efficiency only tells us how well the protein stays on the membrane, we also wanted to determine how functional the protein was for a given immobilization strategy. To test this functionality, each immobilization strategy was tested using the recombinant HA binder as a capture agent for an influenza HA assay. All assays utilized standard antibody-based detection to complete the assay sandwich, in order to focus solely on improvements gained by the immobilization method.

Nitrocellulose strips were prepared with test lines patterned with recombinant flu HA binder as described above. Each flu assay was performed in a dipstick lateral flow format using a 96-well plate pre-loaded with the given assay reagents, and the test strips were manually moved between wells to initiate each assay step. A cellulose absorbent pad (Millipore #CFSP223000) cut to the width of the device and 70 mm tall was secured to the top of the nitrocellulose device to aid wicking, either with tape or with a custom-made plastic housing. Unless otherwise noted, each assay consisted of the following steps: (1) 20 μL recombinant HA or negative control, (2) 20 μL wash, (3) 20 μL mouse anti-HA detection antibody, (4) 20 μL wash, (5) 20 μL gold-conjugated goat-anti-mouse IgG antibody, and (6) 20 μL wash. Recombinant HA was from

one of three influenza strains, as indicated: A/New Caledonia/20/1999 (Protein Sciences, Meriden, CT), A/California/04/2009 (Influenza Reagent Resource (IRR)), or A/Solomon Islands/03/2006 (IRR), all of which are H1N1 strains. Matching detection antibodies were used accordingly. The gold-conjugated secondary (Au-2°) antibody (Au-goat-anti-mouse IgG, Arista Biologicals, Inc., Allentown, PA) was used at optical density (OD) 2.5. All reagents were diluted in a running buffer of PBS or PBST+1 %w/v bovine serum albumin (BSA, Sigma-Aldrich #A7030). Wash buffer was either PBS or PBST, as indicated. The generic assay stack is illustrated in Fig. 2B. After the assay was complete, the wicking pads were removed, and all devices were taped to a standard piece of printer paper and imaged at 48-bit HDR color, 600 dpi, $\gamma=1$ using a desktop scanner (Epson Perfection V700 Photo Scanner).

Signal quantification

All signal intensities from protein lines and test lines were quantified using a custom script in MATLAB (MathWorks, Natick, MA). Using this program, a region of interest (ROI) is drawn semi-manually around the test line of interest, and the average pixel intensity inside this test ROI, I_{test} , is computed. This value is then background-subtracted using the average pixel intensity inside a local background region, I_{bkgd} , and normalized on a scale from 0 to 1 to generate the normalized pixel intensity of the spot, I_{norm} , using Eq. 1.

$$I_{\text{norm}} = \frac{I_{\text{test}} - I_{\text{bkgd}}}{0 - I_{\text{bkgd}}} \quad (1)$$

For each experiment, the channel of the RGB image that was most sensitive to the particular color of signal was chosen for analysis. For the flu HA assays (red color from gold nanoparticles) and the Ponceau S-stained membranes (pink color), the green channel was used. For the Coomassie-stained membranes, the red channel was used. Finally, for the fluorescence images based on FITC-anti-FLAG signal, inverted grayscale quantification was used (signal = white, background = black). In all cases, the normalized pixel intensities represent a range from no signal (0) to maximum possible signal (1).

For the protein spots used in the nitrocellulose-binding anchor protein screening, the area of each protein spot was first determined. Specifically, another custom MATLAB script was used to conduct edge-finding of the spots based on the derivative of pixel intensity, and then fit the edges with ellipses using a least-squares fitting algorithm. The area of each resulting ellipse was then reported as the area of the given protein spot. The average pixel intensity inside this spot area was computed and used to determine the normalized pixel intensity as described by Eq. 1.

For significance testing between two sets of data, the Student's *t* test was used. Unless otherwise specified, a one-tailed, unpaired *t* test assuming unequal variance was applied, with a significance threshold of $\alpha=0.025$. The one-tailed test was chosen to select for unidirectional differences in signal.

Results and discussion

Using the methods outlined above, four immobilization strategies were developed, characterized, and demonstrated using the recombinant flu HA binder as a representative affinity protein. The four immobilization methods, illustrated in Fig. 1, included (1) direct adsorption, (2) covalent attachment of thiolated affinity protein to epoxide-functionalized nitrocellulose, (3) anchoring of biotinylated affinity protein through streptavidin, and (4) genetic fusion of the affinity protein to a custom nitrocellulose-binding anchor protein. Each method was assessed for its immobilization efficiency *via* lateral flow challenge and for its resulting functionality in a lateral flow-based flu HA assay, as illustrated in Fig. 2.

We first characterized the immobilization of the recombinant flu binder under the standard method of direct adsorption. To start, we compared the immobilization efficiency of the flu binder to two commonly used proteins: streptavidin and IgG (see ESM, [Supplementary Results and Discussion](#)). As shown in ESM Fig. S1A, this test revealed that IgG adsorbs robustly and is resistant to desorption under lateral flow challenge, as expected, given its use in lateral flow assays. However, both streptavidin and the flu binder were largely subject to desorption under lateral flow challenge, indicating that not all proteins adsorb to nitrocellulose as robustly as IgG, at least for the standard adsorption conditions tested herein. Moreover, the flu binder was not functional as a capture agent under direct adsorption (ESM Fig. S1B), motivating the development of the three novel methods for recombinant affinity protein immobilization described below.

Covalent attachment of thiolated affinity protein to GMA-modified nitrocellulose is a promising novel strategy for immobilization

Leveraging the customizability of the recombinant flu binder protein, we developed a method of covalently attaching the flu binder to the nitrocellulose assay membrane. This method uses nitrocellulose membrane onto which glycidyl methacrylate (GMA) is grafted through electron beam irradiation [18–20]. This grafting process results in a porous nitrocellulose membrane that is functionalized with epoxide rings, which are highly reactive with thiols. This membrane has many advantages over traditional nitrocellulose and has been used to improve the performance of standard lateral flow immunoassays using IgG capture [unpublished data, in

preparation for publication]. Here, we leveraged the specificity of the GMA functionality for covalent attachment of thiolated proteins. We therefore produced a cysteine-containing mutant of the flu HA binder, resulting in the same affinity protein but with a single, site-specific thiol group for attachment to the GMA-modified nitrocellulose.

To test this covalent attachment method, test lines with HB80.4 or cys-HB80.4 (HB80.4_K315C mutant) were patterned at 100 μM in HBS (+1 mM TCEP for cys-HB80.4 to reduce any disulfide bonds to available thiol groups for reaction with epoxide rings). The flu binders were patterned on both unmodified nitrocellulose (GE FF60,¹ or “NC”) and GMA-modified nitrocellulose (GE FF60-GMA, or “NC-GMA”). As usual, the patterned membranes were dried under desiccation at least overnight and up to 1 week before use.

We used the lateral flow challenge to test the immobilization efficiency of the epoxide-thiol covalent attachment. Challenge solutions of PBS and PBST were used, along with a no lateral flow (LF) control. The protein remaining at each test line was visualized with FITC-anti-FLAG tag staining using the dipstick format and UV imaging method described above. A representative test line for each condition is shown in Fig. 3A, and the normalized pixel intensities are plotted in Fig. 3B as the mean \pm standard deviation (SD) for $n=4$ replicates. These results indicate that both proteins immobilize reasonably well on both regular and GMA-modified nitrocellulose, with the exception of HB80.4 on FF60-GMA. In the case of this GMA-modified nitrocellulose, the thiolated flu binder results in a significantly higher signal after lateral flow challenge with PBST than the regular flu binder ($p<0.025$), indicating that the specific epoxide-thiol attachment works as expected. The direct adsorption of regular HB80.4 to regular FF60 is quite robust here, though, with only minimal loss in signal after the PBST challenge, which is consistent with the previous results described above for this membrane (see Fig. S1, HB80.4 on GE FF60). As expounded above, we know that this HB80.4 protein is not functional when directly adsorbed to FF60, so we next sought to test the functionality of the cys-epoxide attachment method.

We compared the functionality of each protein on each membrane using the flu HA assay described above, with recombinant HA from A/New Caledonia/20/1999 influenza (Protein Sciences #rHA) at 100 nM and accompanying mouse-anti-HA antibody (AbCam #ab66189) at 100 nM. All reagents were diluted in a running buffer of PBS+BSA, and PBS was used for all washes in this experiment. Four replicates were run for each condition, in addition to four replicates of the negative control. A representative test line for one test and one negative control replicate per condition are shown in

¹ GE FF60 has been replaced in the product line with updated FF80HP from GE Healthcare.

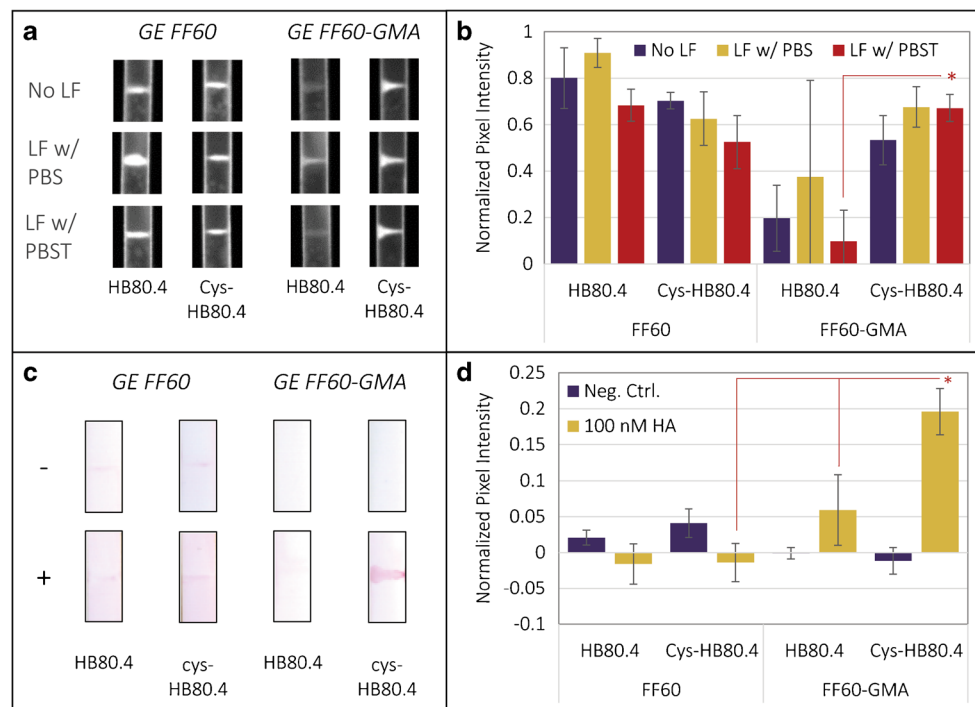


Fig. 3 Covalent attachment of thiolated flu binder to GMA-modified nitrocellulose. **(A)** HB80.4 and cys-HB80.4 visualized on NC and NC-GMA with FITC-anti-FLAG after lateral flow (LF) challenge with PBS and PBST. **(B)** Normalized pixel intensities of the FITC-labeled protein lines, plotted as the mean \pm SD for $n=4$ replicates. *Asterisk* indicates a significantly greater signal intensity for cys-HB80.4 on NC-GMA than HB80.4 ($p<0.025$). **(C)** Flu HA assay signal using HB80.4 and cys-

HB80.4 as capture agents on NC and NC-GMA. Positive test samples (+) were run with 100 nM HA in PBS+BSA, and negative controls (-) were run with PBS+BSA only. **(D)** Normalized pixel intensities of the assay test lines, plotted as the mean \pm SD for $n=4$ replicates. *Asterisk* indicates a significantly greater assay signal for cys-HB80.4 on NC-GMA than for cys-HB80.4 on NC, or for HB80.4 on NC-GMA ($p<0.025$)

Fig. 3C. The normalized pixel intensities are plotted in Fig. 3D as the mean \pm SD for $n=4$ replicates. These results show that only the combination of cys-HB80.4 on FF60-GMA provides a functional assay with test signal significantly greater than that for the negative control ($p<0.025$). Specifically, this signal is significantly greater than that measured for cys-HB80.4 on FF60 and for HB80.4 on FF60-GMA ($p<0.025$), verifying that the specific epoxide-thiol attachment is responsible for the functional assay. Therefore, although the immobilization efficiency does not seem dramatically different, the epoxide-thiol covalent attachment results in the immobilization and display of functional flu binder, yielding a working assay for influenza HA capture and detection. We further improved the functionality by adding a polypeptide linker between the Cys residue and flu binder protein to increase the accessibility of the flu binder for more sensitive capture of HA (see ESM, Supplementary Results and Discussion, Fig. S2).

Overall, this method of covalent attachment echoes previous thiol-based immobilization strategies for other assay substrates [3, 9–11], but, to our knowledge, is the first demonstration on functionalized nitrocellulose membrane. This method represents a promising immobilization technique, given the covalent and site-specific nature of the attachment that allows for the presentation of affinity protein with ideal orientation

and accessibility for binding. However, this system presented high variability in performance with a trend toward decreased signal over time (see ESM, Supplementary Results and Discussion, Fig. S2). This epoxide-thiol approach therefore requires further work to optimize the chemistry for robustness and long-term storage. We also recognize that this method is less feasible for researchers without access to this high level of membrane manipulation, so we sought to develop more broadly applicable techniques as well. These methods are described next.

Immobilization through streptavidin-biotin linkage is effective and enhanced through use of nitrocellulose-binding mutant streptavidin

Streptavidin-biotin linkage is a commonly employed immobilization strategy for biomolecules on assay surfaces, but has not before been optimized for nitrocellulose-based lateral flow assays using nitrocellulose-binding streptavidin mutants and recombinant affinity proteins. Given our ability to site-specifically biotinylate the flu binder through expression with an AVI tag and post-processing with biotin ligase, we sought to explore anchoring of this biotinylated affinity protein with

nitrocellulose-binding mutant streptavidin in order to provide strong, orientation-specific immobilization of the protein.

Since a streptavidin anchor system depends on the direct adsorption of streptavidin to nitrocellulose, we first studied this aspect of the system. Given the previous results shown in Fig. S1A, we knew that streptavidin did not adsorb robustly to nitrocellulose, at least for Millipore HFB135 nitrocellulose. Here, we studied the adsorption of streptavidin to GE FF80HP nitrocellulose and compared it to that of a nitrocellulose-binding mutant version of streptavidin that is available commercially (AbCam #ab51404). While the exact mutation is proprietary and unknown to us, we expected this nitrocellulose-binding mutant streptavidin would adsorb to nitrocellulose more robustly than regular streptavidin and therefore serve as a more effective anchor for biotinylated flu binder.

To test this streptavidin anchor method, test lines with regular streptavidin (“SA”, Thermo Scientific #21125) and mutant streptavidin (“Mut. SA,” AbCam #51404) were patterned at 1 mg/mL in PBS on 3-mm strips of GE FF80HP nitrocellulose.

We first tested the immobilization efficiency of the streptavidin proteins using the lateral flow challenge method.

Challenge solutions of PBS and PBST were used, along with a no lateral flow control. The protein remaining at each test line was visualized using Ponceau S staining, as described above. A representative test line for each condition is shown in Fig. 4A, and the normalized pixel intensities are plotted in Fig. 4B as the mean \pm SD for $n=6$ replicates. These results indicate that the mutant streptavidin adsorbs more robustly to nitrocellulose than regular streptavidin, as expected, with significantly more protein remaining after challenge with PBST for the nitrocellulose-binding mutant streptavidin ($p<0.025$).

Next, we tested the ability of each streptavidin protein to serve as an anchor for biotinylated flu binder (biotin-HB80.4) as a capture agent for the flu HA assay. In this case, the membranes were dried using an alternate drying protocol of 1 h at 37 °C, followed by storage under desiccation overnight before use. Although the drying protocol for this assay experiment was different than the LF challenge experiment, the protocol was held constant for both proteins, making the comparison of performance between the regular and mutant streptavidin anchors valid. The assay was run using recombinant HA from A/New Caledonia/20/1999 influenza (Protein Sciences #rHA) at 100 nM and accompanying mouse-anti-HA antibody (AbCam

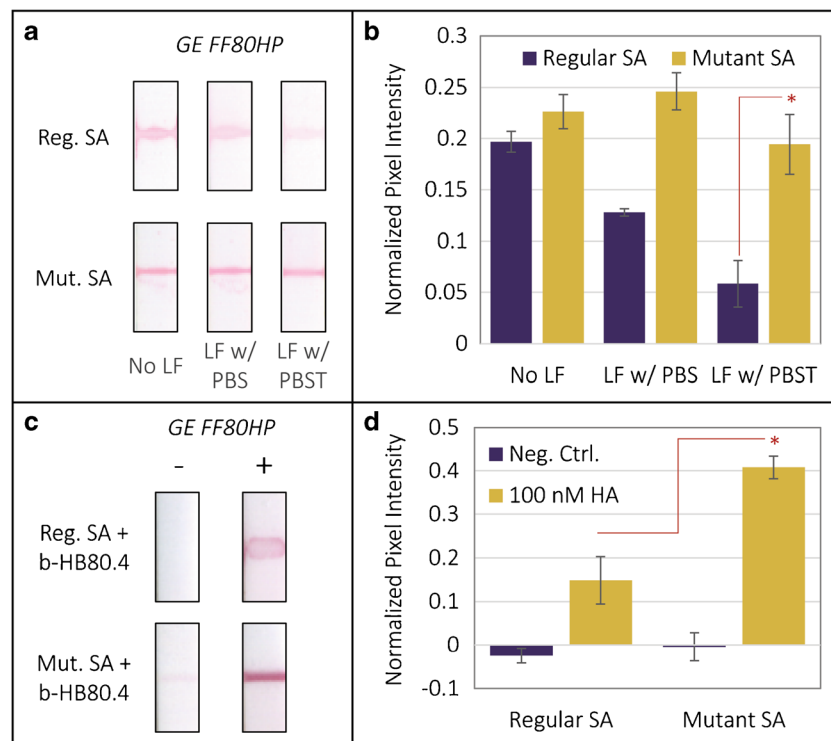


Fig. 4 Immobilization of biotinylated flu binder to nitrocellulose via regular streptavidin (SA) and nitrocellulose-binding mutant SA anchors. (A) Regular and mutant SA visualized on NC with Ponceau S stain after lateral flow (LF) challenge with PBS and PBST. (B) Normalized pixel intensities of the stained protein lines, plotted as the mean \pm SD for $n=6$ replicates. Asterisk indicates a significantly greater signal intensity for mutant SA after challenge with PBST than regular SA ($p<0.025$). (C)

Flu HA assay signal using biotin-HB80.4 anchored by regular and mutant SA on NC. Positive test samples (+) were run with 100 nM HA in PBST+BSA, and negative controls (–) were run with PBST+BSA only. (D) Normalized pixel intensities of the assay test lines, plotted as the mean \pm SD for $n=4$ replicates. Asterisk indicates a significantly greater signal for the mutant SA system than regular SA ($p<0.025$)

#ab66189) at 100 nM. Biotin-HB80.4 was also used at 100 nM. The HA antigen was premixed with biotin-HB80.4 using PBST+BSA as the dilution buffer, while all other reagents were diluted in a running buffer of PBS+BSA. PBS was used for all washes in this experiment. A representative test line for one test and one negative control replicate for each version of streptavidin anchor are shown in Fig. 4C. The normalized pixel intensities are plotted in Fig. 4D as the mean \pm SD for $n=4$ replicates. While the regular streptavidin anchor generates some signal, the test line of the mutant streptavidin anchor is much crisper and darker due to the superior adsorption of this anchor protein to nitrocellulose. Overall, the average pixel intensity of the mutant streptavidin anchor system is greater than that of the regular streptavidin system ($p < 0.025$). Therefore, while regular streptavidin can serve as an anchor for biotinylated affinity reagents on nitrocellulose, the assay performance is enhanced when using the nitrocellulose-binding mutant streptavidin, as expected. While this system yielded a low level of false-positive signal for the negative controls, we eliminated this non-specific signal through the addition of a biotin-BSA wash step (see ESM, Supplementary Results and Discussion, Fig. S3), thereby optimizing this streptavidin-biotin immobilization strategy.

Overall, the mutant streptavidin anchor system for biotinylated affinity proteins performs extremely well for nitrocellulose-based lateral flow assays, providing stronger signal than the covalent epoxide-thiol attachment tested previously. This anchor system is relatively costly, however, requiring the additional expenses of the commercial mutant streptavidin protein, in addition to the enzymatic biotinylation reagents, which offset the advantage of the low cost of the recombinant affinity protein. We therefore explored a fully recombinant alternative to the nitrocellulose-specific streptavidin-biotin system, described next.

Nitrocellulose-binding anchor protein provides close mimic to streptavidin-biotin system at lower cost

In order to develop a lower-cost alternative to the mutant streptavidin-biotin anchoring system, we sought to develop a fusion of the recombinant flu binder protein to a custom nitrocellulose-binding anchor protein. To do so, we first screened several computationally designed proteins for their ability to adsorb robustly to nitrocellulose in order to identify anchor protein candidates. We screened a set of five globular proteins engineered to have ideal energy landscapes and therefore high stability [21], in addition to a 3-helix bundle protein designed to be ultra-stable [22] and have an ideal coating of positive charge, due to its high lysine content (25 % lysine by amino acid). This lysine content confers to the protein a high isoelectric point (pI) of 9.4, which is ideal according to both protein adsorption theory and supporting experimental results

(see ESM, Supplementary Results and Discussion). Of the proteins initially screened, both the Design I (DI) globular protein and the 3-helix bundle protein showed promising adsorption to nitrocellulose, so these were further characterized and compared to IgG, which is known to adsorb robustly. Key properties of the two nitrocellulose-binding anchor protein candidates are summarized in Table 1.

The adsorption of the DI protein, 3-helix protein, and IgG were compared using the lateral flow challenge method. In this case, 0.8-cm-wide strips were used (GE FF80HP nitrocellulose), and proteins were deposited at 1 mg/mL in PBS as spots using 1000 droplets at 450–500 pL per droplet. Red food coloring diluted 1:10 in H₂O was also patterned at the same volume in order to visualize the full wet-out area of that volume. Challenge solutions of PBS and PBST were used, along with a no lateral flow control. The protein remaining at each test spot was visualized using Ponceau S staining, as described above. A representative test spot for each condition is shown in Fig. 5A. The area of each spot relative to the full wet-out area given by the red food coloring is plotted in Fig. 5B as the mean \pm SD for $n=4$ replicates of each protein spot and $n=6$ replicates for the red food coloring control. The normalized green-channel pixel intensity inside each spot is plotted in Fig. 5C as the mean \pm SD for $n=4$ replicates of each protein spot and $n=6$ replicates for the red food coloring control. The small sizes of the protein spots relative to the full wet-out area reveal that all three proteins adsorb to the membrane quickly [16], which is ideal for anchor protein candidates. In fact, the 3-helix protein yields the smallest spot size ($p < 0.025$), indicating that it adsorbs to nitrocellulose the most rapidly. The DI protein yields a spot size similar to IgG (no significant difference), signifying that it also adsorbs quickly to the membrane. All three proteins are also resistant to stripping under lateral flow challenge with PBS and PBST, with no significant difference in the spot intensity relative to the no LF control for the given protein ($p > 0.025$).

Overall, these results indicate that all three proteins adsorb robustly to the nitrocellulose membrane and are strong candidates for nitrocellulose-binding anchor proteins. While this strong adsorption profile was expected for the 3-helix protein, due to its ideal isoelectric point, the strong adsorption of the DI protein was not expected based on its pI alone. We therefore hypothesize that the robust adsorption of the 3-helix and

Table 1 Protein parameters for the two nitrocellulose-binding anchor candidates, 3-helix and DI

	3-helix	DI
PDB Identifier	4TQL	2KL8
Molecular weight	29.6 kDa	10.1 kDa
Isoelectric point	9.4	6.3
Lysine content	25 %	7 %

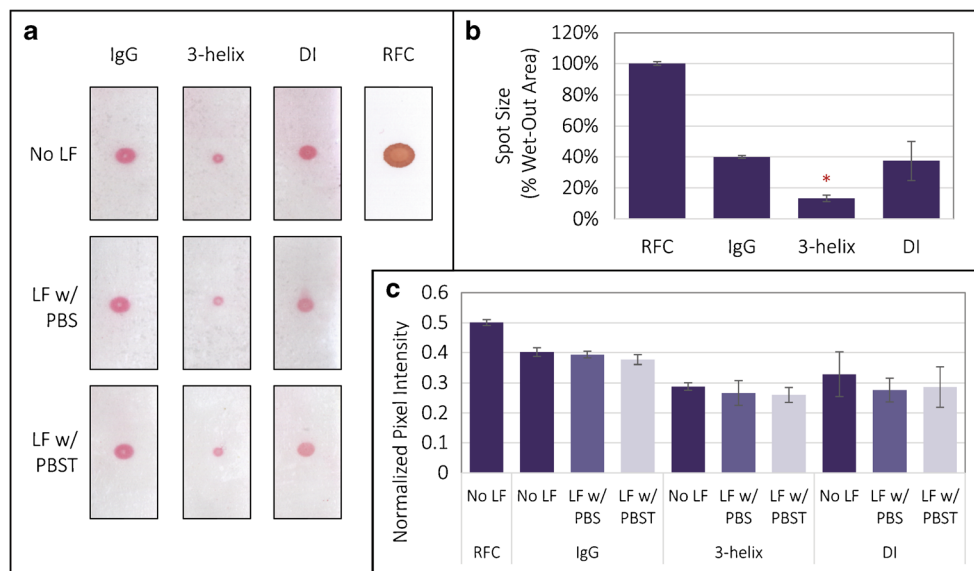


Fig. 5 Screening of the 3-helix and DI nitrocellulose anchor proteins, with comparison to IgG. (A) Protein spots on nitrocellulose (GE FF80HP), subjected to lateral flow (LF) challenge with PBS or PBST or no LF control, and stained with Ponceau S. (B) Spot size relative to the full wet-out area indicated by the red food coloring (RFC), plotted as the

mean±SD for $n=4$ replicates of each protein and $n=6$ replicates of the RFC control. Asterisk indicates that the 3-helix protein exhibits the smallest spot size ($p<0.025$). (C) Normalized pixel intensities of the Ponceau S-stained protein spots after LF challenge, plotted as the mean±SD

DI proteins is partially due to the favorable electrostatics of the systems, in addition to favorable hydrophobic properties that are less well understood (see ESM, Supplementary Results and Discussion for a detailed discussion on this topic and the underlying theory). The theoretical design of anchor proteins like these therefore has much room for improvement and represents an opportune area for future investigation. Nevertheless, our current approach yielded two successful anchor protein candidates, one of which was strongly guided by adsorption theory.

Given the successful adsorption of the 3-helix and DI proteins, we prepared genetic fusions of the stem region flu binder (HB36.6) to each of these nitrocellulose anchor proteins. Unfortunately, the 3-helix-binder fusion protein did not express well in our recombinant expression system and requires

further optimization. The DI-binder fusion protein (DI-HB36.6) did express successfully and was tested for functionality as a capture agent for the flu HA assay on GE FF80HP nitrocellulose. The assay was run using recombinant HA from A/Solomon Islands/03/2006 influenza (Influenza Reagent Resource (IRR) #FR-67) at 10 nM and accompanying mouse-anti-HA antibody (IRR #FR-502) at 100 nM. This DI-HB36.6 fusion system was also compared side-by-side with the optimized mutant streptavidin-biotin system described above, but using the HA and antibody listed here. Additionally, biotin-HB36.5 was used as the biotinylated flu binder for comparison. All reagents were diluted in a running buffer of PBST+BSA, and PBST was used for all washes in this experiment. A representative test line for one test and one negative control replicate for each assay system are shown in Fig. 6A. The

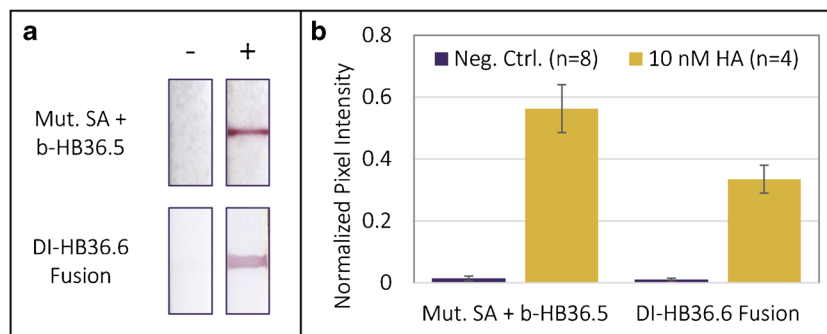


Fig. 6 Comparison of the mutant SA-biotin and DI fusion protein anchoring methods for HB36 as a capture agent in the flu HA assay on GE FF80HP nitrocellulose. (A) Flu HA assay signal using biotin-HB36.5 anchored by mutant SA versus using the DI-HB36.6 fusion protein. Positive test samples (+) were run with 10 nM HA in PBST+BSA, and

negative controls (−) were run with PBST+BSA only. (B) Normalized pixel intensities of the assay test lines, plotted as the mean±SD for $n=4$ replicates of the test concentration (10 nM HA) and $n=8$ replicates of the negative control

normalized pixel intensities are plotted in Fig. 6B as the mean \pm SD for $n=4$ replicates for the test samples and $n=8$ replicates for the negative controls.

These results indicate that the DI-binder fusion serves as an effective capture agent for the flu HA assay, producing a strong signal for the test sample and a clean negative control. The average pixel intensity of the test line for the DI-binder fusion system is lower than that of the mutant streptavidin-biotinylated binder system, however, indicating that latter system produces the most functional assay ($p<0.025$). This loss in signal may be due to the lower degree of control of the orientation of the affinity protein for the fusion protein system as compared to the streptavidin anchor system. More specifically, since the fusion protein is immobilized by direct adsorption, it is subject to random orientation, which likely results in a portion of the affinity protein that is adsorbed binding-site-down and is therefore unavailable for capture of the incoming antigen. Despite this partial loss in signal intensity, the recombinant fusion protein system is approximately 1000 times cheaper than the nitrocellulose-specific streptavidin-biotin system ($\sim\$0.0006/\text{test}$ versus $\sim\$0.4845/\text{test}$), thereby offering good performance at a much lower cost. The high cost for the mutant streptavidin system—which is due to the high costs of the commercial mutant streptavidin protein and biotinylation reagents—would likely be partially mitigated by the purchase of bulk reagents for at-scale production, but is expected to remain significantly more expensive. The choice in immobilization system for any given assay will therefore depend on the sensitivity and cost restraints at play. While the statistical limits of detection were not calculated for the proof-of-concept assays demonstrated here, understanding this difference in analytical sensitivity for a given assay, as well as the clinically required detection limit, would be the next step for an assay developer in assessing this choice of immobilization system. If both systems have sufficient sensitivity for the given application, then cost could be minimized by using the fusion protein system. However, if the utmost sensitivity is required for a given application then the nitrocellulose-specific streptavidin-biotin system may be the preferred choice, if the higher cost can be supported.

Paper-based influenza hemagglutinin assay using recombinant flu binder with nitrocellulose-specific streptavidin-biotin attachment outperforms traditional immunoassay

Given the superior performance of the nitrocellulose-specific streptavidin-biotin anchoring system to the other methods developed herein, we sought to compare this novel immobilization system to the gold standard immunoassay method of IgG capture by direct adsorption. Since commercial lateral flow tests do not exist for HA detection (all commercial influenza

rapid diagnostic tests detect the internal nucleoprotein instead), we developed the standard IgG-based lateral flow strips in-house. To do so, an antibody binding pair was determined from the IgG antibodies available from the IRR for HA from A/Solomon Islands/3/2006 influenza. The capture antibody (IRR #FR-503) was patterned onto GE FF80HP nitrocellulose at 0.5 mg/mL in PBS (stock concentration) in the form of test lines, as described above. The detection antibody (IRR #FR-502) was conjugated directly to gold nanoparticles using a commercial conjugation kit (InnovaCoat Gold 40 nm Gold Particle Kit, #230-0005, InnovaBiosciences, Cambridge, United Kingdom). The assay was run through the sequential delivery of the following reagents: (1) 20 μ L HA at 10 nM or negative control, (2) 20 μ L PBST wash, (3) 20 μ L gold-conjugated detection antibody at OD 2.5, and (4) 20 μ L PBST wash. All reagents were diluted in a running buffer of PBST+BSA. This assay was compared side-by-side with the mutant streptavidin-biotin system, performed using biotin-HB36.5 at 100 nM, A/Solomon Islands/3/2006 HA at 10 nM, and the same gold-conjugated detection antibody as above. Here, the biotinylated binder and HA were premixed

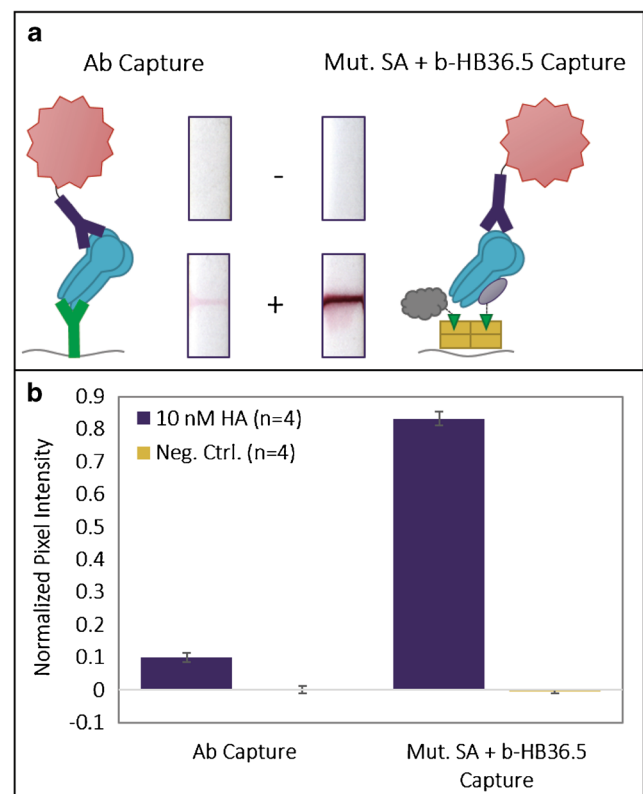


Fig. 7 Comparison of the novel mut. SA+b-HB36.5 capture system for the flu HA assay to a traditional Ab capture system. GE FF80HP nitrocellulose was used in both cases. (A) Flu HA assay signal for each system, in addition to an illustration of each assay stack. Positive test samples (+) were run with 10 nM HA in PBST+BSA, and negative controls (-) were run with PBST+BSA only. (B) Normalized pixel intensities of the assay test lines, plotted as the mean \pm SD for $n=4$ replicates

prior to flow, and a biotin-BSA wash was used for the first wash step. The gold-conjugated detection antibody was then added sequentially, followed by the final PBST wash. In doing so, this test provided a comparison of the novel nitrocellulose-specific streptavidin-biotin immobilization system developed herein to the gold standard of IgG capture by direct adsorption, using the same exact detection system in order to focus solely on the impact of the capture agent and immobilization method.

A representative test line for one test and one negative control replicate for each assay system are shown in Fig. 7A. The normalized pixel intensities are plotted in Fig. 7B as the mean \pm SD for $n=4$ replicates of each condition. These results show that the combination of the recombinant affinity protein with the mutant streptavidin-biotin anchor system provides much stronger assay signal than the use of standard IgG capture by direct adsorption ($p<0.025$). Overall, this work not only demonstrates the use of novel immobilization methods for capture agents on nitrocellulose, but also illustrates the improvements in assay functionality that can be made by using these methods.

Conclusion

This work represents novel efforts to immobilize affinity reagents to nitrocellulose membrane for use in paper-based assays. While this work was done using a computationally designed affinity protein, these methods can be applied to any recombinant affinity protein (e.g., scFv and other antibody-derived protein fragments) or modified protein (e.g., IgG antibody that has been biotinylated or reduced/thiolized). Therefore, even the immobilization of IgG itself could be improved through these more sophisticated and controlled immobilization techniques.

Recombinantly expressed or modified proteins provide many options for attachment to the assay substrate. Here, we have focused on nitrocellulose membranes, which are the most commonly used materials for lateral flow tests, but the assessment methods shown here could be applied to other assay substrates as well. We found that direct adsorption was not an effective strategy for all affinity proteins—as evidenced by our small flu binder—despite the fact that it is the mainstay of antibody immobilization for traditional lateral flow immunoassays. Covalent attachment through epoxide-thiol linkage is a novel method that takes advantage of the customizability of the affinity protein and a new modified nitrocellulose membrane. This method, while promising, requires further optimization, including careful attention to the chemistry of the buffers used and the storage conditions. Attachment through the well-known streptavidin-biotin linkage is extremely effective and enhanced by the use of a commercially available mutant version of streptavidin specifically designed to bind

to nitrocellulose. However, the high cost of this commercial product creates an added expense that counteracts the financial advantage of using recombinant affinity proteins instead of antibodies. Lower-cost alternatives represent an important area of future work. As an intermediate solution, the nitrocellulose anchor protein that we employed here represents one alternative to the streptavidin-biotin system, although closer mimics could be developed to improve attachment and binding functionality. While each method has its benefits and drawbacks, the nitrocellulose-specific streptavidin-biotin system yielded the overall strongest signal for the influenza HA assay. This system resulted in improved assay performance compared to the traditional method of IgG antibody directly adsorbed to nitrocellulose membrane.

Overall, we have demonstrated that the novel immobilization methods presented herein for recombinant affinity proteins can be used to improve paper-based assay performance. Future work remains to assess further details of these systems, such as sample matrix effects, buffer optimization, blocking agent optimization, and long-term storage. Nevertheless, the demonstration of these proof-of-concept assays represents a significant step forward in the development of paper-based assays. With this work, we aim to broaden the toolset available to the paper-based diagnostics community and spur continued innovation in the field.

Acknowledgments The authors thank colleagues in the Yager, Baker, and GE Global Research groups for helpful discussions regarding this work. The authors particularly acknowledge Rashmi Ravichandran for her help in producing many of the recombinant flu binder proteins. This material is based upon work supported by the National Science Foundation Graduate Research Fellowship Program under Grant No. DGE – 0718124, by the National Institute of Allergy and Infectious Diseases of the National Institutes of Health under award number R01AI096184, and by the University of Washington Department of Bioengineering. The content is solely the responsibility of the authors and does not necessarily represent the official views of the National Institutes of Health.

Conflict of interest The authors declare that they have no conflict of interest.

References

1. Tonkinson JL, Stillman BA (2002) Nitrocellulose: a tried and true polymer finds utility as a post-genomic substrate. *Front Biosci* 7: c1–c12
2. Fridley GE, Holstein CA, Oza SB, Yager P (2013) The evolution of nitrocellulose as a material for bioassays. *MRS Bull* 38:326–330. doi:10.1557/mrs.2013.60
3. Gubala V, Harris LF, Ricco AJ, Tan MX, Williams DE (2012) Point of care diagnostics: status and future. *Anal Chem* 84:487–515. doi:10.1021/ac2030199
4. Mansfield M (2009) Nitrocellulose membranes for lateral flow immunoassays: a technical treatise. In: Wong RC, Tse HY (eds) *Lateral flow immunoass.* Humana Press, New York, pp 95–113

5. O'Farrell B (2009) Evolution of lateral flow-based immunoassay systems. In: Wong RC, Tse HY (eds) *Lateral flow immunoassay*. Humana Press, New York, pp 1–33
6. Vermasvuori R (2009) Production of recombinant proteins and monoclonal antibodies—techno-economical evaluation of the production methods. Helsinki University of Technology. <http://lib.tkk.fi/Lic/2009/um100121.pdf>
7. Fleishman SJ, Whitehead TA, Ekiert DC, Dreyfus C, Corn JE, Strauch E-M, Wilson IA, Baker D (2011) Computational design of proteins targeting the conserved stem region of influenza hemagglutinin. *Science* 332:816–821. doi:10.1126/science.1202617
8. Whitehead TA, Chevalier A, Song Y, Dreyfus C, Fleishman SJ, De Mattos C, Myers CA, Kamisetty H, Blair P, Wilson IA, Baker D (2012) Optimization of affinity, specificity and function of designed influenza inhibitors using deep sequencing. *Nat Biotechnol* 30: 543–548. doi:10.1038/nbt.2214
9. Wu P, Castner DG, Grainger DW (2008) Diagnostic devices as biomaterials: a review of nucleic acid and protein microarray surface performance issues. *J Biomater Sci Polym Ed* 19:725–753. doi:10.1163/156856208784522092
10. Rusmini F, Zhong Z, Feijen J (2007) Protein immobilization strategies for protein biochips. *Biomacromolecules* 8:1775–1789. doi:10.1021/bm061197b
11. Jonkheijm P, Weinrich D, Schröder H, Niemeyer CM, Waldmann H (2008) Chemical strategies for generating protein biochips. *Angew Chem Int Ed* 47:9618–9647. doi:10.1002/anie.200801711
12. Pelton R (2009) Bioactive paper provides a low-cost platform for diagnostics. *TrAC Trends Anal Chem* 28:925–942. doi:10.1016/j.trac.2009.05.005
13. Sicard C, Brennan JD (2013) Bioactive paper: biomolecule immobilization methods and applications in environmental monitoring. *MRS Bull* 38:331–334. doi:10.1557/mrs.2013.61
14. Yu A, Shang J, Cheng F, Paik BA, Kaplan JM, Andrade RB, Ratner DM (2012) Biofunctional Paper via the Covalent Modification of Cellulose. *Langmuir* 28:11265–11273. doi:10.1021/la301661x
15. Yetisen AK, Akram MS, Lowe CR (2013) Paper-based microfluidic point-of-care diagnostic devices. *Lab Chip* 13:2210. doi:10.1039/c3lc50169h
16. Holstein CA, Fridley GE, Adcock CA, Yager P (2015) Methods and Models to Examine Protein Adsorption to Nitrocellulose. *Anal Chem* (in review)
17. Metkar SS, Mahajan SK, Sainis JK (1995) Modified procedure for nonspecific protein staining on nitrocellulose paper using Coomassie brilliant blue R-250. *Anal Biochem* 227:389–391. doi:10.1006/abio.1995.1297
18. Li B, Olsen CE, Moore DR (2011) Porous membranes having a polymeric coating and methods for their preparation and use. US patent application, US20130171618 A1
19. Li B, Olsen CE, Moore DR (2011) Porous membranes having a polymeric coating and methods for their preparation and use. US patent application, US20130171368 A1
20. Li B, Olsen CE, Moore DR (2011) Porous membranes having a polymeric coating and methods for their preparation and use. US patent application, US20130171026 A1
21. Koga N, Tatsumi-Koga R, Liu G, Xiao R, Acton TB, Montelione GT, Baker D (2012) Principles for designing ideal protein structures. *Nature* 491:222–227. doi:10.1038/nature11600
22. Huang P-S, Oberdorfer G, Xu C, Pei XY, Nannenga BL, Rogers JM, DiMaio F, Gonen T, Luisi B, Baker D (2014) High thermodynamic stability of parametrically designed helical bundles. *Science* 346:481–485. doi:10.1126/science.1257481
23. Currie LA (1995) Nomenclature in evaluation of analytical methods including detection and quantification capabilities (IUPAC Recommendations 1995). *Pure Appl Chem* 67:1699–1723. doi:10.1351/pac199567101699
24. Holstein CA, Griffin M, Hong J, Sampson PD (2015) A statistical method for determining and comparing limits of detection of bioassays. *Anal Chem*. doi:10.1021/acs.analchem.5b02082
25. Van Oss CJ, Good RJ, Chaudhury MK (1987) Mechanism of DNA (Southern) and protein (Western) blotting on cellulose nitrate and other membranes. *J Chromatogr* 391:53–65
26. American Chemical Society, American Chemical Society (1995) *Proteins at interfaces II: fundamentals and applications*. American Chemical Society, Washington, DC
27. EMD Millipore Corporation (2008) *Rapid lateral flow test strips: consideration for product development*. EMD Millipore Corporation, Billerica, MA
28. Přistoupil TI, Kramlová M, Štěrbíková J (1969) On the mechanism of adsorption of proteins to nitrocellulose in membrane chromatography. *J Chromatogr A* 42:367–375. doi:10.1016/S0021-9673(01)80636-1